Hard superconducting nitrides

Xiao-Jia Chen*, Viktor V. Struzhkin*, Zhigang Wu*, Maddury Somayazulu†, Jiang Qian‡, Simon Kung*§, Axel Nørlund Christensen¶, Yusheng Zhao‡, Ronald E. Cohen*, Ho-kwang Mao*, and Russell J. Hemley*‖

*Geophysical Laboratory, Carnegie Institution of Washington, Washington, DC 20015; †Advanced Photon Source, Argonne National Laboratory, Argonne, IL 60439; ‡Los Alamos Neutron Science Center Division, Los Alamos National Laboratory, Los Alamos, NM 87545; §Department of Chemistry, California Institute of Technology, MSC 593, Pasadena, CA 91126; and ¶Højkolvej 7, DK-8210 Aarhus V, Denmark

Contributed by Russell J. Hemley, January 7, 2005

Detailed study of the equation of state, elasticity, and hardness of selected superconducting transition-metal nitrides reveals interesting correlations among their physical properties. Both the bulk modulus and Vickers hardness are found to decrease with increasing zero-pressure volume in NbN, HfN, and ZrN. The computed elastic constants from first principles satisfy $c_{11} > c_{12} > c_{44}$ for NbN, but $c_{11} > c_{44} > c_{12}$ for HfN and ZrN, which are in good agreement with the neutron scattering data. The cubic δ-NbN superconducting phase possesses a bulk modulus of 348 GPa, comparable to that of cubic boron nitride, and a Vickers hardness of 20 GPa, which is close to sapphire. Theoretical calculations for NbN show that all elastic moduli increase monotonically with increasing pressure. These results suggest technological applications of such materials in extreme environments.

elasticity | elastic constants | equations of state | hardness | binary compounds

Hard superconducting materials are of considerable interest for specific electronic applications. Superconductivity has been discovered in diamond, generally believed to be the hardest material having very high shear and bulk moduli (1, 2), with a superconducting transition temperature (T_c) near 4 K when doped with boron (3). However, the transition-metal compounds having the sodium chloride (*B*1) structure (e.g., NbN, NbC, ZrN, or HfN) are also hard superconductors but with relatively higher T_cs. The transition temperatures of solid solutions of NbN and NbC can reach a maximum value of 17.8 K, which is close to those found for the cubic A15-type compounds such as Nb_3Sn and V_3Si (4). The refractory characteristics of these transition-metal nitrides and carbides have been applied as coatings to increase the wear resistance, for instance, in cutting tools as well as for magnetic storage devices. The unusual hardness enhancement in these materials has been theoretically shown to originate from a particular σ-band of bonding states between the nonmetal *p* orbitals and the metal *d* orbitals that strongly resists shearing strains (5). At the moment, there is a need to investigate elastic and mechanical properties of these superconductors under simulated extreme working conditions.

Here, we report both experimental and theoretical studies of the equation of state, elasticity, and hardness of selected superconducting transition-metal nitrides. We find that the cubic δ-NbN superconducting phase possesses a bulk modulus of 348 GPa, comparable to that of cubic boron nitride, and a Vickers hardness of 20 GPa, which is close to sapphire (Al_2O_3) (6). The results indicate that these nitrides are good candidates for engineering hard superconducting materials.

Experimental and Theoretical Details

Equations of state studies were based on angle-dispersive synchrotron powder x-ray diffractometry with a diamond anvil cell. The diffraction experiments were carried out at the synchrotron beam line 16ID-B of the Advanced Photon Source High Pressure Collaborative Access Team. A 500×500-μm^2 monochromatic beam of wavelength $\lambda = 0.4219$ Å was focused by using a pair of bimorph mirrors to a 10×12-μm^2 beam. The diffraction data were recorded on a MAR345 imaging plate and integrated by using FIT2D software (7). The geometric parameters and the wavelength were calibrated by using a silicon standard (NIST 640c standard). Powder samples were loaded into a hole in stainless-steel gaskets with a nominal diameter of 100 μm and 10- to 15-μm thickness between two 400-μm-diameter flat diamond culets. A ruby chip served as an optical pressure sensor in the diamond anvil cell (8). LiF was chosen as a pressure medium for NbN, and silicon oil was used as a pressure medium in the HfN and ZrN samples. The powder samples with grain sizes <2 μm were obtained by crushing the single crystals of NbN, HfN, and ZrN. Single crystals grown by the zone-annealing technique have been detailed (9–11). Hardness measurements were performed on the nitride single crystals by means of a Vickers indentation method with a pyramidal diamond indenter.

The thermodynamical stability of these transition-metal nitrides are examined by first-principles calculations. All calculations are based on the density functional theory within the local density approximation. We used a planewave basis and pseudopotentials with the ABINIT (version 4.3.2) package (12) to optimize structures and calculate total energies and electronic structures. The OPIUM program (13) was used to generate pseudopotentials for N, Nb, Zr, and Hf. Plane-wave basis sets with a cut-off of 50 Ha were tested and found to be highly converged. A dense $16 \times 16 \times 16$ **k**-point mesh was used over the Brillouin zone.

The elastic moduli of these transition-metal nitrides were calculated from stress (σ) changes caused by very small strain (ε) through the relation $c_{ij} = \sigma_i/\varepsilon_j$ (14). Cubic crystals have only three independent elastic constants, namely c_{11}, c_{12}, and c_{44}, for the *B*1 structure. The bulk modulus K_0 was calculated from fitting energy and volume data to the Vinet equation of state (15).

Results and Discussion

X-ray diffraction patterns of NbN were taken up to 51.2 GPa. Typical patterns taken in the course of increasing pressure are shown in Fig. 1. The ambient pressure phase for NbN is *fcc*, as evidenced by the observations of (111), (200), (220), (311), and (222) peaks, and the measured lattice parameter is $a_0 = 4.379(2)$ Å. The (111) peak of LiF shifts much faster than the (200) peak of NbN under pressure, almost overlapping at 30 GPa but separating again at 51.2 GPa. At high pressures, the same diffraction peaks still remain, indicating that there is no phase transformation up to 51.2 GPa. The measured lattice parameter at 51.2 GPa is 4.213(3) Å, which corresponds to a volume compression V/V_0 of 0.89.

Fig. 2 shows the measured pressure-volume curve or equation of state for NbN, HfN, and ZrN samples to 51.2 GPa at room temperature. The experimental data were fitted to the Vinet equation of state (16)

$$P = \frac{3K_0(1-x)}{x^2} \exp\left[\frac{3}{2}(K_0' - 1)(1-x)\right], \qquad [1]$$

with $x = (V/V_0)^{1/3}$, where V_0 and V are the zero-pressure and compressed volumes and K_0 and K_0' represent the bulk modulus at

‖To whom correspondence should be addressed. E-mail: r.hemley@gl.ciw.edu.

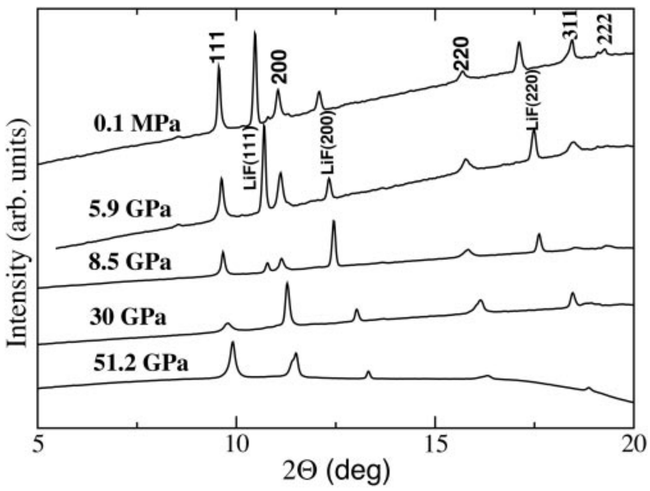

Fig. 1. Angle-dispersive x-ray diffraction patterns of NbN at various pressures up to 51.2 GPa in a diamond-anvil cell. LiF was used as a pressure medium. The pressures indicated were measured by the ruby fluorescence technique.

Table 1. Summary of the zero-pressure elastic constants c_{ij}, shear modulus G, Poisson's ratio ν, Young's modulus E in the (111) and (001) directions, bulk modulus K_0, and its pressure derivative K_0' in cubic NbN, HfN, and ZrN obtained from first-principles calculations and neutron scattering measurements (9–11)

	NbN		HfN		ZrN	
Moduli	Theory	Neutron	Theory	Neutron	Theory	Neutron
c_{11} (GPa)	739	608	694	679	611	471
c_{12} (GPa)	161	134	112	119	117	88
c_{44} (GPa)	76	117	134	150	129	138
G (GPa)	161	165	197	202	176	160
ν	0.18	0.18	0.14	0.15	0.16	0.16
E_{111} (GPa)	212	309	336	387	351	341
E_{001} (GPa)	682	560	579	644	663	443
K_0 (GPa)	354	292	306	306	285	215
K_0'	4.36		4.21		4.28	

The elastic constants determined from neutron data have limited accuracy (10–15%).

zero pressure and its pressure derivative. Metals with simple $B1$ NaCl structure always have a characteristic K_0' of ~4.0 (17). Taking K_0' of 4.0 for our samples, we obtained the bulk moduli at ambient condition of 348, 260, and 248 GPa for NbN, HfN, and ZrN, respectively. The bulk modulus was found to decrease with increasing zero-pressure volume V_0 from 83.98(11) Å^3 for NbN through 93.14(14) Å^3 for HfN to 95.69(9) Å^3 for ZrN. Our calculated values of K_0 are 354, 306, and 285 GPa for NbN, HfN, and ZrN, respectively. The K_0 obtained from the fits to the static data are close to our calculated results and previous theoretical predictions (18, 19). The calculated zero-pressure volumes are 82.26, 87.94, and 92.28 Å^3 for NbN, HfN, and ZrN, respectively. These values agree with our experimental results at ambient pressure. Note that the bulk modulus for NbN is comparable to that of the superhard material cubic boron nitride (6).

The elastic moduli were obtained from a linear fit by the stress-strain relation. For cubic lattices, the Poisson's ratio ν can be expressed as $\nu = c_{12}/(c_{11} + c_{12})$ (20). The computed results of these parameters for cubic NbN, HfN, and ZrN at ambient condition are listed in Table 1. We also estimated the elastic

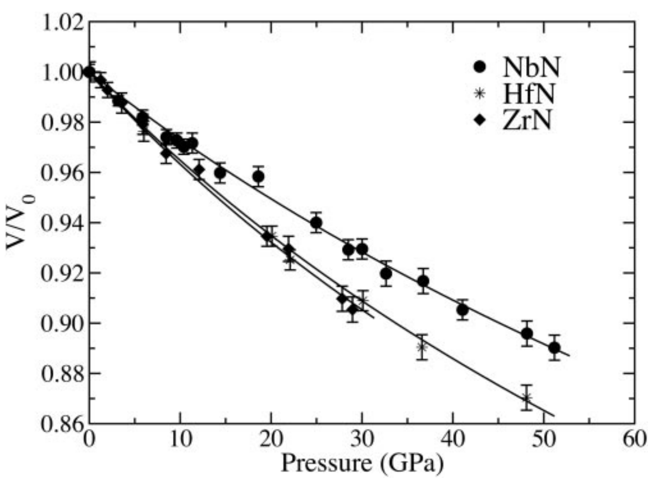

Fig. 2. Pressure-volume data for transition-metal nitrides. The zero-pressure volumes (V_0) are 83.98(11), 93.14(14), and 95.69(9) Å^3 for NbN, HfN, and ZrN, respectively. The solid lines are the Vinet fits to the measured data. The characteristic K_0' of 4.0 is used in fitting the data.

moduli from the initial slopes of the dispersion curves obtained from neutron scattering data (9–11). The results also are presented in Table 1 for comparison. As can be seen, the first-principles calculations and neutron scattering measurements give a qualitatively similar tendency of the three elastic constants in these materials. That is, $c_{11} > c_{12} > c_{44}$ for NbN, but $c_{11} > c_{44} > c_{12}$ for HfN and ZrN. The obtained elastic moduli in HfN are in excellent agreement for both methods. However, the value of c_{11} obtained from first-principles calculations is larger than that from neutron scattering measurements in NbN and ZrN. Both methods give an almost constant Poisson's ratio of ~0.16 for these nitrides. It is worth noting that the calculated values of K_0' are consistent with the value of 4.0 characteristic of many materials.

The Young's and shear moduli (E and G) are two important quantities for technological and engineering applications and provide fundamental description of a material's mechanical behavior. The former is defined as the ratio between stress and strain. The latter, which is related to bond bending, depends on the nature of the bond and decreases as a function of ionicity. For the compound to have a high shear modulus and high hardness, directional bonding and a rigid structural topology are typically required. The shear modulus G can be calculated from the Viogt approximation [$G = (c_{11} - c_{12} + 3c_{44})/5$]. Notice that in the cubic system the Young's modulus E is not isotropic (20). The variation with direction depends on $(l_1^2 l_2^2 + l_2^2 l_3^2 + l_3^2 l_1^2)$ with l_i being the unit vector. The quantity is zero for the directions of the cube axes (001) and has its maximum value of 1/3 in the (111) direction. In the cubic nitrides, the Young's modulus is a minimum for the (111) and a maximum for (001) directions. In Table 1, we also summarized these parameters obtained from the resulting elastic constants. Both the first-principles calculations and neutron scattering measurements provide a consistent estimation of the Young's and shear moduli for these nitrides.

We investigated theoretically the high-pressure behavior of the elastic moduli for cubic δ-NbN. Fig. 3*a* shows the pressure dependence of the elastic constants. All constants increase monotonically with increasing pressure. These elastic constants satisfy the generalized elastic stability criteria for cubic crystals under hydrostatic pressure (21), $c_{11} + c_{12} > 0$, $c_{44} > 0$, and $c_{11} - c_{12} > 0$. The first criterion is closely related to the bulk modulus, which is obviously necessary for stability. The latter two are thought to play a more subtle role since c_{44} involves shearing the metal-N bonds and $c_{11} - c_{12}$ involves stretching (and compression) of the metal-N bonds with a combination of bending and stretching of metal–metal bonds. We

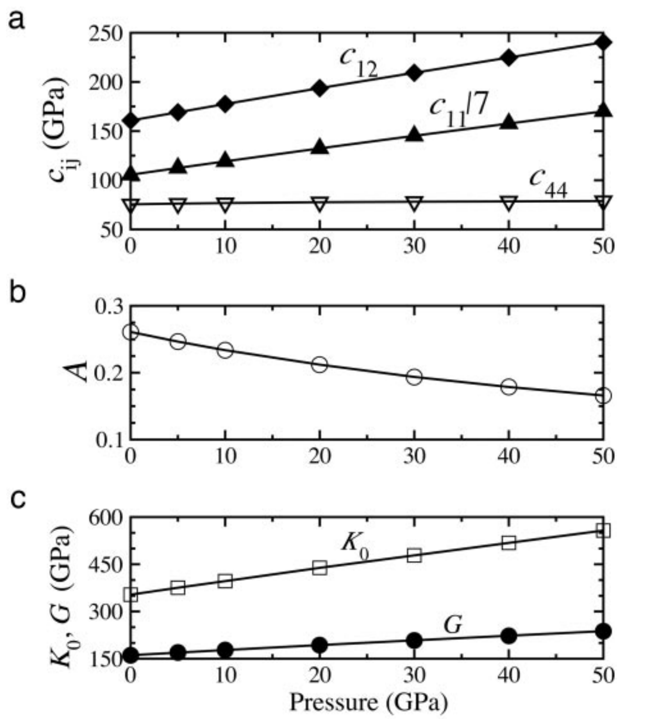

Fig. 3. Pressure dependence of the elastic constants c_{ij} (*a*), the elastic anisotropy A (*b*), and the bulk modulus K_0 and shear modulus G (*c*) in cubic δ-NbN.

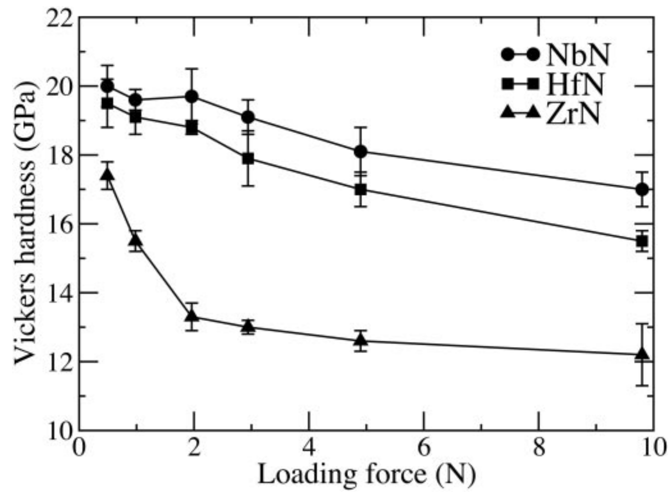

Fig. 4. Vickers hardness of the transition-metal nitrides NbN, HfN, and ZrN single crystals as a function of the loading force.

note that the inequality $c_{11} > c_{12} > c_{44}$ is satisfied over a wide pressure range (i.e., to 50 GPa).

The elastic anisotropy at high pressure is important for understanding the evolution of bonding in the system. A measure of the anisotropy of the elasticity is $A = 2c_{44}/(c_{11} - c_{12})$ for cubic crystals. For isotropic elasticity, the two shear moduli $(c_{11} - c_{12})/2$ and c_{44} are equal and the anisotropy becomes unity. In Fig. 3*b* we plotted the pressure dependence of A for cubic δ-NbN. A shows a gradual decrease with increasing pressure. The rapid increase of c_{11} with pressure is expected because of enhanced nearest-neighbor interaction, which leads to a stretching of the metal-N bonds $(c_{11} - c_{12})$. On the other hand, pressure induces $sp \rightarrow d$ electron transfer from N to Nb atoms (22), giving rise to the occupation of σ-bonding states derived from *d–d* interactions. This band is lowered under shear strain (5), which gives a modest negative contribution to c_{44}. As a result, the pressure-induced decrease of A is dominated by stretching of the metal-N bonds rather than the gradual shearing of the structure.

Aggregate values for the bulk K_0 and shear G modulus were obtained from the individual elastic constants (Fig. 3*c*). The bulk modulus increases with pressure and reaches 557 GPa at pressure of 50 GPa. At 20 GPa, the bulk modulus of δ-NbN reaches the zero-pressure value of the bulk modulus of diamond (1). The shear modulus also increases across the whole pressure range. The behavior of the moduli suggests an increasing hardness in this material with pressure.

Using conventional microhardness testing techniques, the Vickers hardness H_V was measured under a loading force from 0.49 to 9.8 N. The loading time was fixed at 15 s. Fig. 4 shows the measured H_V for the studied transition-metal nitrides under various loads. From the results, it can be seen that the hardness decreases with increasing lattice parameter. The average hardness values are 20.0, 19.5, and 17.4 GPa under a load of 0.49 N for NbN, HfN, and ZrN, respectively. For comparison, our measured H_V of 20 GPa for cubic δ-NbN is slightly lower than the reported ≈23 GPa in a δ-$NbN_{0.93}$ film (23). The measured H_V of 15.5 GPa in HfN under a loading force of 9.8 N is very close to the reported H_V^{10N} of 14.5 GPa in HfN ceramics (24). Another observation of our results is that the Vickers hardness decreases with the increase in load. Similar behavior has been reported for cubic boron nitride and Al_2O_3 (25). Note that the cubic δ-NbN superconducting phase has a the bulk modulus of 348 GPa, comparable to that of cubic boron nitride, and a Vickers hardness of 20 GPa, the same as sapphire. Recent studies in films (23) revealed that the hardness of the hexagonal δ′-NbN phase with high nitrogen concentration can reach to 40 GPa. The relatively large bulk modulus and high hardness in the superconducting cubic δ-NbN phase are favorable for potential hard-device applications.

NbN has the highest T_c among the transition-metal nitrides. Currently, NbN films are being examined in applications of radio frequency superconducting accelerator cavities (26), superconducting quantum interference devices (27), superconducting hot-electron photodetectors (28), and IR sensors (29). Our results reveal that this material is highly incompressible compared with HfN and ZrN because of its high values of the bulk modulus and Vickers hardness. Application of pressure increases both the bulk and shear moduli. The enhancement of hardness is therefore expected under high pressure. Meanwhile, T_c was found to increase with pressure in this compound (30). These combined features make NbN a good candidate along with hard superconductors, such as boron-doped diamond, for possible applications under extreme conditions.

Work at the Carnegie Institution was supported by U.S. Department of Energy Grant DEFG02-02ER4595, Office of Naval Research Grant N000140210506, the Department of Energy/Office of Basic Energy Sciences, Department of Energy/National Nuclear Security Administration, Carnegie/Department of Energy Alliance Center Grant DE-FC03-03N00144, the National Aeronautics and Space Administration, the National Science Foundation, and the W. M. Keck Foundation. Work at the Los Alamos National Laboratory was performed under the auspices of the Department of Energy. The High-Pressure Collaborative Access Team is a collaboration involving the Carnegie Institution of Washington, Lawrence Livermore National Laboratory, the University of Hawaii, the University of Nevada Las Vegas, and the Carnegie/Department of Energy Alliance Center at the Argonne National Laboratory.

1. Occelli, F., Loubeyre, P. & Letoullec, R. (2003) *Nat. Mater.* **2,** 151–154.
2. Yan, C. S., Mao, H. K., Li, W., Qian, J., Zhao, Y. S. & Hemley, R. J. (2004) *Phys. Stat. Sol. A* **201,** 25–27.
3. Ekimov, E. A., Sidorov, V. A., Bauer, E. D., Mel'nik, N. N., Curro, N. J., Thompson, J. D. & Stishov, S. M. (2004) *Nature* **428,** 542–545.
4. Matthias, B. T. (1953) *Phys. Rev.* **92,** 874–876.
5. Jhi, S. H., Ihm, J., Louie, S. G. & Cohen, M. L. (1999) *Nature* **399,** 132–134.
6. Haines, J., Léger, J. M. & Bocquillon, G. (2001) *Annu. Rev. Mater. Res.* **31,** 1–23.
7. Hammersley, A. P., Svensson, S. O., Hanfland, M., Fitch, A. N. & Häusermann, D. (1996) *High Press. Res.* **14,** 235–248.
8. Mao, H. K., Xu, J. A. & Bell, P. M. (1986) *J. Geophys. Res.* **91,** 4673–4676.
9. Christensen, A. N., Dietrich, O. W., Kress, W., Teuchert, W. D. & Currat, R. (1979) *Solid State Commun.* **31,** 795–799.
10. Christensen, A. N., Kress, W., Miura, M. & Lehner, N. (1983) *Phys. Rev. B* **28,** 977–981.
11. Christensen, A. N., Dietrich, O. W., Kress, W. & Teuchert, W. D. (1979) *Phys. Rev. B* **19,** 5699–5703.
12. Gonze, X., Beuken, J. M., Caracas, R., Detraux, F., Fuchs, M., Rignanese, G. M., Sindic, L., Verstraete, M., Zerah, G., Jollet, F., *et al*. (2002) *Comput. Mater. Sci.* **25,** 478–492.
13. Rappe, A. M., Rabe, K. M., Kaxiras, E. & Joannopoulos, J. D. (1990) *Phys. Rev. B* **41,** 1227–1230.
14. Nielsen, O. H. & Martin, R. M. (1983) *Phys. Rev. Lett.* **50,** 697–700.
15. Cohen, R. E., Gülseren, O. & Hemley, R. J. (2000) *Am. Mineral.* **85,** 338–344.
16. Vinet, P., Ferrante, J., Rose, J. H. & Smith, J. R. (1987) *J. Geophys. Res.* **92,** 9319–9325.
17. Bridgman, P. W. (1945) *Proc. Am. Acad. Arts Sci.* **76,** 1–7.
18. Hart, G. L. W. & Klein, B. M. (2000) *Phys. Rev. B* **61,** 3151–3154.
19. Stampfl, C., Mannstadt, W., Asahi, R. & Freeman, A. J. (2001) *Phys. Rev. B* **63**, 155106, 1–11.
20. Nye, J. F. (1957) *Physical Properties of Crystals* (Clarendon, Oxford).
21. Wang, J. H., Yip, S., Phillpot, S. R. & Wolf, D. (1993) *Phys. Rev. Lett.* **71,** 4182–4185.
22. Palanivel, B., Kalpana, G. & Rajagopalan, M. (1993) *Phys. Stat. Sol. B* **176,** 195–202.
23. Benkahoul, M., Martinez, E., Karimi, A., Sanjinés, R. & Lévy, F. (2004) *Surf. Coat. Technol.* **180–181,** 178–183.
24. Desmaison-Brut, M., Montintin, J., Valin, F. & Boncoeur, M. (1994) *J. Eur. Ceram. Soc.* **13,** 379–386.
25. He, D. W., Zhao, Y. S., Daemen, L., Qian, J., Shen, T. D. & Zerda, T. W. (2002) *Appl. Phys. Lett.* **81,** 643–645.
26. Benvenuti, C., Chiggiato, P., Parrini, L. & Russo, R. (1993) *Nuclear Instru. Methods Phys. Res. A* **336,** 16–22.
27. Faucher, M., Fournier, T., Pannetier, B., Thirion, C., Wernsdorfer, W., Villegier, J. C. & Bouchiat, V. (2002) *Physica C* **368,** 211–217.
28. Lindgren, M., Currie, M., Zeng, W. S., Sobolewski, R., Cherednichenko, S., Voronov, B. & Gol'tsman, G. N. (1998) *Appl. Supercond.* **6,** 423–428.
29. Durand, D., Dalrymple, B., Eaton, L., Spargo, J., Wire, M., Dowdy, M. & Ressler, M. (1999) *Appl. Supercond.* **6,** 741–750.
30. Chen, X. J., Struzhkin, V. V., Kung, S., Mao, H. K., Hemley, R. J. & Christensen, A. N. (2004) *Phys. Rev. B* **70**, 014501, 1–6.

APPLIED PHYSICAL SCIENCES